

Linearly Polarized Gravitational Waves from Bubble Collisions

Katarina Trailović^{1,2,*}

¹*Jožef Stefan Institute, Jamova cesta 39, 1000 Ljubljana, Slovenia*

²*Faculty of Mathematics and Physics, University of Ljubljana, Jadranska ulica 19, 1000 Ljubljana, Slovenia*

Physics beyond the Standard Model may give rise to first-order phase transitions proceeding via the nucleation of vacuum bubbles, whose subsequent collisions generate gravitational waves (GWs). Their detection would open the possibility of investigating the universe in its first instants. If the transition is slow enough, such that it completes with the nucleation and collision of only two bubbles, the resulting GW signal is linearly polarized. We show that in this case triangular interferometers such as LISA and the Einstein Telescope could be able to not only measure the magnitude of the GW but also establish its linear polarization. This would give a strong hint about the origin of the signal.

INTRODUCTION

Future triangular gravitational-wave (GW) detectors such as the Einstein Telescope (ET) and LISA will provide improved sensitivity to GW polarizations, surpassing what is achievable with current networks of ground-based interferometers [1–4]. Their multiple, non-coaligned arms and long-baseline modulation will enable a more precise reconstruction of the two tensor polarizations predicted in general relativity (GR), as well as stringent tests for additional modes. This capability represents a major advance over existing two- and three-detector networks, for which incomplete baseline coverage and limited signal-to-noise typically restrict the ability to isolate polarization content.

Accurate measurements of GW polarizations open a new observational window to test fundamental physics. On the one hand, they allow powerful constraints on theories that extend GR and predict extra scalar or vector polarizations [5–8]. On the other hand, even within GR, the polarization state of a GW encodes valuable information about its source. While most astrophysical and cosmological processes generate stochastic backgrounds that are unpolarized on average, notable exceptions exist. For example, axion–gauge-field inflation can produce chiral (circularly polarized) gravitational waves through the amplification of a single helicity mode [9, 10]. Such scenarios highlight the possibility that polarization may serve as a diagnostic tool for identifying specific early-Universe mechanisms otherwise inaccessible to direct observation.

In this work, we propose a new mechanism for producing linearly polarized gravitational waves in the early Universe. It has long been understood that collisions of true-vacuum bubbles in first-order phase transitions release substantial energy in the form of gravitational waves, making such transitions among the most promising sources of potentially detectable signals [11–15]. New physics beyond the Standard Model can give rise to first-order phase transitions in the early Universe. We demonstrate that if such transitions proceed sufficiently slowly

to complete through the nucleation and collision of only two vacuum bubbles, the resulting GW signal would exhibit a linear polarization. Using analytical estimates, we further show that slow transitions of this type can occur and successfully complete. Importantly, this would produce a distinctive and potentially observable signature in future GW detectors, indicative of the unusual dynamics underlying this type of phase transition.

COLLISION OF TWO SPHERICAL BUBBLES

In the following, we compute the GW polarization tensor generated by the collision of two spherical bubbles, adopting the analytic formalism of Refs. [13, 16, 17].

The linearized Einstein equations in the Lorentz gauge, $\partial^\nu \bar{h}_{\mu\nu} = 0$, take the form $\square \bar{h}_{\mu\nu} = -(16\pi G/c^4)T_{\mu\nu}$, where $\bar{h}_{\mu\nu} = h_{\mu\nu} - \eta_{\mu\nu}h/2$ is the trace-reversed metric perturbation. In vacuum, this reduces to the wave equation $\square \bar{h}_{\mu\nu} = 0$. Exploiting residual gauge freedom, one can impose the transverse-traceless (TT) gauge, $h^{0\mu} = 0$, $h^i_i = 0$, $\partial^j h_{ij} = 0$, which isolates the two physical polarization states of the gravitational wave.

For a plane wave $h_{\mu\nu}$ in the Lorentz gauge, the transformation to the TT gauge is obtained via the projection $h_{ij}^{\text{TT}} = \Lambda_{ij,kl} h_{kl}$, where $\Lambda_{ij,kl} = P_{ik}P_{jl} - P_{ij}P_{kl}/2$ and $P_{ij} = \delta_{ij} - \hat{k}_i \hat{k}_j$. The general plane-wave solution is $h_{ij}^{\text{TT}} = e_{ij}(\mathbf{k}) e^{ik_\mu x^\mu}$, where $k^\mu = (\omega, \omega \hat{\mathbf{k}})$ satisfies the null condition $k^\mu k_\mu = 0$.

For a propagation direction $\hat{\mathbf{k}} = (\sin \theta, 0, \cos \theta)$, the transversality condition $\hat{k}^i h_{ij}^{\text{TT}} = 0$ implies $\sin \theta h_{1j} + \cos \theta h_{3j} = 0$. Combining this with the traceless condition and defining $h_+ \equiv h_{11}$ and $h_\times \equiv h_{12}$, we obtain the general polarization tensor,

$$e_{ij}(\mathbf{k}) = \begin{pmatrix} h_+ & h_\times & -\tan \theta h_+ \\ h_\times & -(1 + \tan^2 \theta) h_+ & -\tan \theta h_\times \\ -\tan \theta h_+ & -\tan \theta h_\times & \tan^2 \theta h_+ \end{pmatrix}, \quad (1)$$

representing a GW in TT gauge propagating along $\hat{\mathbf{k}} = (\sin \theta, 0, \cos \theta)$ with the two independent polarization modes h_+ and h_\times .

Now, let us calculate h_{ij}^{TT} in the case of two spherical bubbles colliding. Far from the source, we have

$$h_{ij}^{\text{TT}}(t, \mathbf{x}) = \frac{1}{r} \frac{4G}{c^5} \Lambda_{ij,kl}(\hat{k}) \int \frac{d\omega}{2\pi} \tilde{T}_{kl}(\omega, \mathbf{k}) e^{-i\omega(t-r/c)}, \quad (2)$$

where $\mathbf{x} = \hat{\mathbf{k}} \cdot r$ and $r \gg d$, with d being the diameter of the source. Also, \tilde{T}_{kl} is the Fourier transform of the stress-energy tensor, whose spatial part takes the form $T_{ij} = \partial_i \phi \partial_j \phi - \mathcal{L} \delta_{ij}$. Since $\Lambda_{ij,kl} \delta_{kl} = 0$, we will ignore the part proportional to δ_{ij} and take

$$\tilde{T}_{ij}(\omega, \mathbf{k}) = \int dt \int d^3x \partial_i \phi \partial_j \phi e^{i\omega t - i\mathbf{k} \cdot \mathbf{x}}. \quad (3)$$

Considering that our problem is axially symmetric about the z axis connecting the two bubble centers, we can take, without loss of generality, $\hat{\mathbf{k}} = (\sin \theta, 0, \cos \theta)$. Then, axial symmetry and fixing $\hat{k}_y = 0$ implies $\tilde{T}_{xy}(\omega, \mathbf{k}) = \tilde{T}_{yz}(\omega, \mathbf{k}) = 0$. Therefore, we obtain

$$\Lambda_{ij,kl}(\hat{k}) \tilde{T}_{kl}(\omega, \mathbf{k}) = \begin{pmatrix} X & 0 & -\tan \theta X \\ 0 & -(1 + \tan^2 \theta) X & 0 \\ -\tan \theta X & 0 & \tan^2 \theta X \end{pmatrix}, \quad (4)$$

with $X = 1/2 \cos^2 \theta (\tilde{T}_{xx} \cos^2 \theta - \tilde{T}_{yy} + \tilde{T}_{zz} \sin^2 \theta - 2\tilde{T}_{xz} \sin \theta \cos \theta)$. Comparing this matrix with the general parametrization in (1), we see that $h_{\times} = 0$. Hence, in the case of two spherical bubbles colliding, only the h_{+} polarization is generated.

EARLY UNIVERSE BUBBLES

We want to assess how likely it is that first order phase transitions in the early universe could have completed after nucleating only two bubbles leading to the emission of linearly polarized GWs.

We consider the phase transition to occur after inflation, during the radiation-dominated epoch, where the scale factor evolves as $a \propto t^{1/2}$ and the energy density is given by $\rho = \pi^2 g_{\star} T^4/30$. The Friedmann equation, $H^2 = 8\pi\rho/3M_p^2$, then implies the scaling relation $t \propto T^{-2}$ between cosmic time and temperature.

In this regime, finite-temperature (thermal) tunneling dominates over quantum tunneling, as the presence of a thermal bath enhances the decay probability of the false vacuum. The decay rate can thus be written as [18, 19]

$$\Gamma(T) = T^4 \left(\frac{S_3}{2\pi T} \right)^{3/2} e^{-S_3/T}, \quad (5)$$

where S_3 is the three-dimensional Euclidean action of the $O(3)$ -symmetric bounce configuration.

To study the decay rate in a model-independent manner, we parameterize it as $\Gamma(t) = C(t)e^{-A(t)}$. Expanding around the completion time t_{\star} , we obtain $A(t) \simeq$

$A_{\star} - \beta(t - t_{\star})$, where $\beta \simeq \dot{\Gamma}/\Gamma$ characterizes the inverse duration of the phase transition. It is convenient to introduce the dimensionless parameter $\beta_H = \beta/H(t_{\star})$, which compares the transition timescale with the Hubble rate.

In contrast to the conventional approach, we do not characterize the phase transition timescale using the standard percolation time. The motivation for adopting a different completion criterion is that our framework requires the transition to end in a two-bubble regime, where the dynamics are driven exclusively by the nucleation and subsequent expansion of only two bubbles. We therefore define the effective completion time t_{\star} as the moment at which the false-vacuum survival probability has dropped to the percent level, imposing the stricter condition $\mathcal{P}_{\text{FV}}(t_{\star}) = e^{-I(t_{\star})} \simeq 0.01$, where [20–22]

$$I(t) = \frac{4\pi}{3} \int_{t_c}^t dt' \Gamma(t') a(t')^3 r(t, t')^3 \quad (6)$$

is the expected volume of true-vacuum bubbles per unit volume of space at time t , $r(t, t') = \int_{t'}^t dt'' v_w/a(t'')$ is the comoving radius at time t of a bubble nucleated at t' propagating with wall velocity v_w and t_c is the critical time at which the true and false vacuum are degenerate.

As we are interested in slow phase transitions that on average nucleate only two bubbles before completion, we must ensure that the total false-vacuum volume, $\mathcal{V}_{\text{FV}}(t) \propto a(t)^3 \mathcal{P}_{\text{FV}}(t)$, decreases with time as the transition completes. This requires that the rate of true-vacuum conversion exceeds the dilution from cosmic expansion, implying [23]

$$\frac{1}{\mathcal{V}_{\text{FV}}} \frac{d\mathcal{V}_{\text{FV}}}{dt} = 3H - \frac{dI}{dt} < 0, \quad (7)$$

at the time of completion.

The expected number of bubbles nucleated up to time t within one Hubble volume is given by [24]

$$N(t) = \frac{4\pi}{3} \int_{t_c}^t dt' \frac{\Gamma(t') \mathcal{P}_{\text{FV}}(t')}{H(t')^3} \quad (8)$$

where $\mathcal{P}_{\text{FV}}(t)$ accounts for the false-vacuum fraction to avoid counting bubbles nucleated within already converted regions.

In the radiation-dominated era, the completion time can be written as $t_{\star} = \beta_H/(2\beta)$. Since thermal tunneling dominates in this regime, the prefactor scales as $C(t) \propto T^4 \propto t^{-2}$, and we therefore take $C(t) = \tilde{C} \cdot t^{-2}$ in the following. Furthermore, taking $t_c \simeq 0$ ¹ for analytic

¹ Setting $t_c = x t_{\star}$ with $x \in [0, 1)$, we find that the maximum value occurs at $x = 0.026$, corresponding to the mean bubble number reaching $N = 3$ already for $\beta_H = 1$. Thus, only for $x \in [0, 0.026)$ a range of $\beta_H > 1$ exists fulfilling $2 \leq N < 3$. This bound is tied to the slow-transition regime: the transition

simplicity, we obtain

$$I(t_*) = \frac{32\pi B_* e^{-\beta_H/2}}{3\beta_H^2} \left(-4 - 2e^{\beta_H/2}(-2 + \beta_H) + 6\beta_H + \sqrt{2\pi}(-3 + \beta_H) \sqrt{\beta_H} \operatorname{erfi}\left(\sqrt{\beta_H/2}\right) \right) \quad (9)$$

and

$$N(t_*) = \frac{32\pi B_*}{3v_w^3\beta_H^2} \int_0^{\beta_H} dx x \exp \left[\frac{x-\beta_H}{2} + \frac{32\pi B_*}{3\beta_H^2} \cdot \left(4 - 6x + 2e^{\frac{x}{2}}(x-2) + \sqrt{2\pi}x(3-x) \operatorname{erfi}\sqrt{\frac{x}{2}} \right) \right], \quad (10)$$

where we defined $B_* \equiv \tilde{C} t_*^3 v_w^3$. Imposing $I(t_*) = 4.6$, which encodes a 1% false-vacuum survival probability, and employing Eq. (9), one directly obtains B_* . Consequently, Eq. (7) depends only on β_H and we verified that for any $\beta_H \geq 1$ the inequality holds, meaning that completion at this time t_* is ensured. Also, Eq. (10) is now only a function of β_H and v_w and we require that, by the completion of the phase transition, on average two bubbles have nucleated, i.e., $2 \leq N(t_*) < 3$. This condition yields, for each v_w , an allowed range of β_H . For the case $v_w/c = 1$, we find $3.48 \leq \beta_H < 5.22$ and for smaller wall velocities the allowed ranges of β_H are shown in Fig. 1.

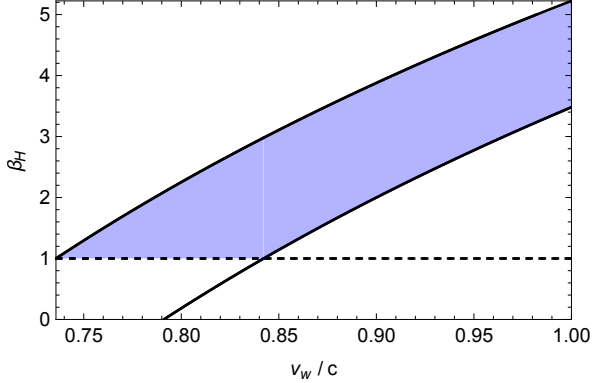


FIG. 1. Range of the inverse phase-transition duration, β_H , for which the expected number of bubbles at completion is two, shown as a function of the bubble wall velocity v_w (purple region). The dashed line indicates $\beta_H = 1$; below this value, nucleation proceeds more slowly than the cosmic expansion, implying that the bubble wall velocity must satisfy $v_w/c > 0.74$.

The mean bubble size R_* at the time of collision sets the characteristic length scale of the source and thus

determines the peak frequency, amplitude, and overall shape of the resulting GW spectrum. In the scenario where two bubbles fill the entire Hubble volume, the mean bubble radius at collision can be approximated as $R_* H_* = 0.5$. This estimate can be verified by explicitly computing the mean bubble radius, which at a given time t is given by [25]

$$R_*(t) = \frac{1}{a^3(t)n_B(t)} \int_{t_c}^t dt' \Gamma(t') a^3(t') \mathcal{P}_{\text{FV}}(t') R(t, t'), \quad (11)$$

where $n_B(t)$ is the bubble density, defined as

$$n_B(t) = \frac{1}{a^3(t)} \int_{t_c}^t dt' \Gamma(t') a^3(t') \mathcal{P}_{\text{FV}}(t') \quad (12)$$

and $R(t, t')$ is the physical size of a bubble at time t which was nucleated at time t' , i.e. $R(t, t') = a(t)r(t, t')$.

From the preceding analysis, the ratio of the mean bubble size to the Hubble radius at the completion time t_* can be expressed as a function of v_w and β_H , as shown in Fig. 2. The figure indicates that $R_* H_*$ at completion is approximately 0.5, implying that bubble collisions occur at a time close to t_* . This supports the consistency of adopting $R_* H_* = 0.5$ as a representative value at the time of collision.

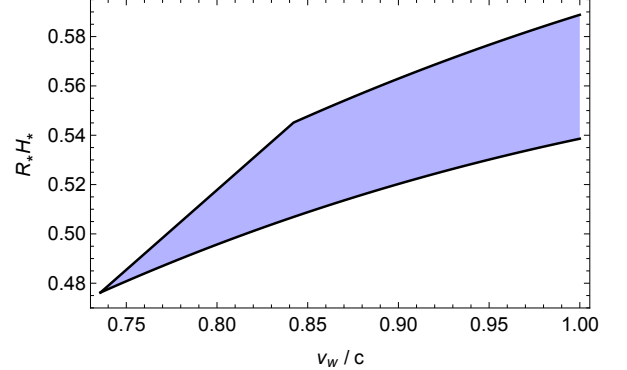


FIG. 2. Ratio of the mean bubble size to the Hubble radius at the completion time as a function of the wall velocity v_w . The upper (lower) black line corresponds to the lower (upper) bound of β_H , for which the expected number of bubbles at completion is two. The shaded purple region indicates the allowed values of $R_* H_*$, with β_H increasing from top to bottom within the permitted range.

Note that in this regime the nucleated bubbles have radii comparable to the Hubble scale. Consequently, gravitational effects on the bounce action can no longer be neglected. Thus, a first-principles computation of a concrete microscopic model exhibiting such a slow phase transition would require replacing the flat-space Euclidean action S_3 in Eq. (5) by its gravitationally corrected counterpart, i.e. the action obtained from the Coleman–De Luccia bounce [26]. However, our analysis is entirely model-independent, meaning that the parameter

duration admits two consistent estimates, $\tau \sim 1/\beta = 2t_*/\beta_H$ and $\tau \sim t_* - t_{\text{nuc}} \lesssim t_* - t_c = t_*(1-x)$, where $t_{\text{nuc}} > t_c$ is the time of nucleation, leading to the parametric relation $2/\beta_H \lesssim (1-x)$ and for slow transitions $2/\beta_H \sim \mathcal{O}(1)$, implying $(1-x) \sim \mathcal{O}(1)$ for self-consistency.

β_H is treated as an effective quantity, and should therefore be understood as already encoding any gravitational corrections relevant in this slow-transition regime.

GW SIGNAL

Having determined the duration of the phase transition and the mean bubble radius at the time of collision, for a transition that completes after the nucleation of two bubbles, our next goal is to evaluate the strength of the resulting GW signal and assess its detectability with future triangular GW detectors.

There are three processes that contribute to the stochastic GW background:

$$\frac{d\Omega_{\text{GW}}h^2}{d\ln f} \simeq \frac{d\Omega_\phi h^2}{d\ln f} + \frac{d\Omega_{\text{sw}}h^2}{d\ln f} + \frac{d\Omega_{\text{turb}}h^2}{d\ln f}, \quad (13)$$

the collisions of bubble walls, sound waves and magneto-hydrodynamic turbulence in the plasma after collision.

The GW power spectrum today coming from bubble-wall collisions was found by numerical simulations to be the following fitting function [27]

$$\begin{aligned} \frac{d\Omega_\phi h^2}{d\ln k} &\simeq 3.22 \times 10^{-3} (H_\star R_\star)^2 \left(\frac{\kappa_\phi \alpha}{1 + \alpha} \right)^2 F_{\text{GW}}^0 \\ &\times \frac{(a+b)^c \tilde{k}^b k^a}{(b\tilde{k}^{(a+b)/c} + a k^{(a+b)/c})^c}, \end{aligned} \quad (14)$$

where $\alpha = \rho_{\text{vac}}/\rho_{\text{rad}}^\star$ is the ratio of the vacuum energy density released during the phase transition to the radiation bath, $\rho_{\text{rad}}^\star = g_\star \pi^2 T_\star^4/30$ with g_\star the number of relativistic degrees of freedom in the plasma at T_\star . $\kappa_\phi = \rho_\phi/\rho_{\text{vac}}$ is the fraction of vacuum energy density that gets converted into the gradient energy of the scalar, $\tilde{k} = 3.2/R_\star$ is the peak and $a = 3$, $b = 1.51$, $c = 2.18$. Also, the redshifting factor is given by

$$F_{\text{GW}}^0 = 1.67 \times 10^{-5} \left(\frac{100}{g_\star} \right)^{1/3}. \quad (15)$$

Thus we obtain

$$\begin{aligned} \frac{d\Omega_\phi h^2}{d\ln f} &\simeq 5 \times 10^{-8} (H_\star R_\star)^2 \left(\frac{\kappa_\phi \alpha}{1 + \alpha} \right)^2 \left(\frac{100}{g_\star} \right)^{1/3} \\ &\times \frac{(a+b)^c \tilde{f}^b f^a}{(b\tilde{f}^{(a+b)/c} + a f^{(a+b)/c})^c}. \end{aligned} \quad (16)$$

The peak frequency generated by the bubble collision today is

$$\begin{aligned} \tilde{f}_\phi^0 &= \left(\frac{a_\star}{a_0} \right) \frac{3.2}{2\pi R_\star} \\ &\simeq 1.65 \times 10^{-5} \text{Hz} \left(\frac{T_\star}{100 \text{GeV}} \right) \left(\frac{g_\star}{100} \right)^{1/6} \frac{3.2}{2\pi R_\star H_\star}. \end{aligned} \quad (17)$$

The acoustic sound-wave contribution is given by [28]

$$\begin{aligned} \frac{d\Omega_{\text{sw}}h^2}{d\ln f} &\simeq 2.061 F_{\text{GW}}^0 \left(\frac{\kappa_{\text{sw}} \alpha}{1 + \alpha} \right)^2 (H_\star R_\star) \tilde{\Omega}_{\text{GW}} \\ &\times \left(\frac{f}{\tilde{f}_{\text{sw}}} \right)^3 \left(\frac{7}{4 + 3(f/\tilde{f}_{\text{sw}})^2} \right)^{7/2}, \end{aligned} \quad (18)$$

where $\tilde{\Omega}_{\text{GW}} = 1.2 \times 10^{-2}$ from simulations and $\kappa_{\text{sw}} = \rho_{\text{sw}}/\rho_{\text{vac}}$ the fraction of vacuum energy that gets transformed into bulk motion of the fluid. The peak frequency of the sound-wave spectrum today is

$$\tilde{f}_{\text{sw}}^0 \simeq 4.46 \times 10^{-6} \text{Hz} \left(\frac{T_\star}{100 \text{GeV}} \right) \left(\frac{g_\star}{100} \right)^{1/6} \frac{\beta}{v_w H_\star} \frac{\tilde{k} R_\star}{10}, \quad (19)$$

where \tilde{k} is the angular peak frequency of the sound-wave spectrum.

Finally, the contribution from magneto-hydrodynamic turbulence in the plasma can be modeled as [29]

$$\begin{aligned} \frac{d\Omega_{\text{turb}}h^2}{d\ln f} &= 3.35 \times 10^{-4} \left(\frac{H_\star}{\beta} \right) \left(\frac{\kappa_{\text{turb}} \alpha}{1 + \alpha} \right)^{3/2} \left(\frac{100}{g_\star} \right)^{1/3} \\ &\times v_w \frac{\left(f/\tilde{f}_{\text{turb}} \right)^3}{\left(1 + f/\tilde{f}_{\text{turb}} \right)^{11/3} (1 + 8\pi f/h_\star)}, \end{aligned} \quad (20)$$

where $\kappa_{\text{turb}} = \rho_{\text{turb}}/\rho_{\text{vac}}$ and the inverse Hubble time at GW production, redshifted today,

$$h_\star = 1.65 \times 10^{-5} \text{Hz} \left(\frac{T_\star}{100 \text{GeV}} \right) \left(\frac{g_\star}{100} \right)^{1/6}. \quad (21)$$

The turbulence peak frequency today is

$$\tilde{f}_{\text{turb}}^0 \simeq 2.7 \times 10^{-5} \text{Hz} \frac{1}{v_w} \left(\frac{\beta}{H_\star} \right) \left(\frac{T_\star}{100 \text{GeV}} \right) \left(\frac{g_\star}{100} \right)^{1/6}. \quad (22)$$

We assume that the bubbles are in the run-away regime and hence we parametrize [29]

$$\kappa_\phi = \frac{\alpha - \alpha_\infty}{\alpha}, \quad \kappa_{\text{sw}} = \frac{\alpha_\infty^2}{\alpha(0.73 + 0.083\sqrt{\alpha_\infty + \alpha_\infty})} \quad (23)$$

and $\kappa_{\text{turb}} = 1 - \kappa_\phi - \kappa_{\text{sw}}$, where $\alpha_\infty < \alpha$ corresponds to the onset of the runaway regime, in which the driving pressure from the released vacuum energy surpasses the frictional force from the surrounding plasma, leading to indefinite acceleration of the bubble walls towards the speed of light.

In Fig. 3, we present the total stochastic GW background coming from a radiation-dominated phase transition along with its individual contributions, computed for the parameters $\alpha = 0.5$ (solid) and $\alpha = 0.8$ (dashed),

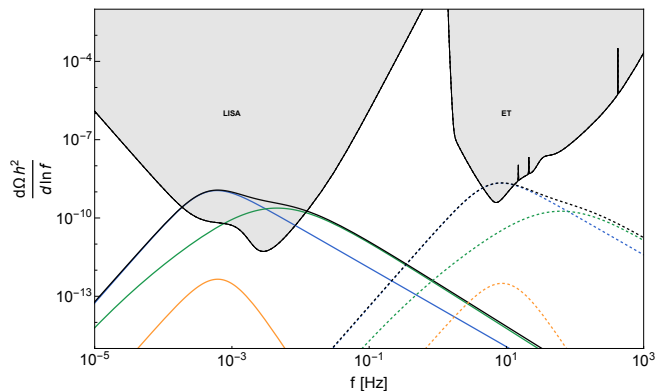


FIG. 3. Total stochastic GW background (black) from a radiation-dominated phase transition and its individual contributions from bubble-wall collisions (blue), sound waves (orange), and hydrodynamic turbulence (green), for $\alpha = 0.5$, $T_* = 3.6 \times 10^3$ GeV (solid) and $\alpha = 0.8$, $T_* = 5.0 \times 10^3$ GeV (dashed). The projected sensitivity curves of the future detectors LISA and Einstein Telescope (ET) are shown as grey regions.

$\alpha_\infty = 0.05$, $T_* = 3.6 \times 10^3$ GeV (solid) and $T_* = 5.0 \times 10^7$ GeV (dashed), $g_* = 100$, $v_w = 0.95$ and $\tilde{k}R_* = 10$, with β_H chosen at the midpoint of the allowed range.

For this choice of parameters, the resulting GW spectrum falls within the sensitivity band of LISA and the Einstein Telescope (ET) respectively. In particular, the contribution from bubble-wall collisions—corresponding to the linearly polarized component—lies within LISA’s and ET’s detectable range, whereas the sound-wave and turbulence contributions, which are expected to be non-polarized, are subdominant and can even fall outside the detectability range. The peak of the bubble-collision component remains within the LISA band for transition temperatures T_* between 5.5×10^2 GeV and 1.5×10^5 GeV and within the ET band for T_* between 2.5×10^7 GeV and 1.0×10^8 GeV. Varying the bubble-wall velocity v_w does not qualitatively affect this result. Similarly, increasing α within the range $0.5 < \alpha \leq 1$ slightly raises the peak amplitude, but the variation remains within one order of magnitude. In contrast, smaller values of α lead to a faster suppression of the peak amplitude, potentially causing the signal to drop below LISA’s or ET’s sensitivity range. Changing α_∞ modifies the relative contributions from bubble-wall collisions, sound waves, and turbulence.

We also note that the axial symmetry of the two-bubble collision geometry enforces an angular dependence in the GW amplitude: it vanishes along the axis connecting the two bubble centers, peaks in the orthogonal plane, and remains nonzero at intermediate angles [13]. Since exact alignment occupies zero solid angle on the sphere, it occurs with probability zero; thus, a null signal is not realized for any generic observation di-

rection. This projection factor can be absorbed into the phase-transition strength parameter, α , without loss of generality.

For a supercooled scenario ($\alpha > 1$), the resulting GW signal would be even stronger [23, 30–40]. However, as discussed in the Appendix, it is unlikely that a supercooled phase transition can complete through the nucleation of only two bubbles; in this regime, successful completion typically requires the nucleation of many bubbles. Nevertheless, in finely tuned scenarios it may still be possible for the transition to complete with only two.

POLARIZATION DETECTION

In the previous section, we have seen that the GWs emitted from a two bubble collision at completion could be detected by future experiments. The special feature of this scenario is the production of linearly polarized GWs.

Detecting this polarization pattern requires sensitivity to both GW tensor modes, achievable either through a network of at least three non-coaligned detectors or by a single triangular interferometer. Current ground-based interferometers such as the Advanced Virgo, Advanced KAGRA and the two Advanced LIGO detectors can as a joint network separate the polarizations, though the precision is limited by geometry and signal-to-noise ratio [3–5]. Future triangular detectors, including the Einstein Telescope and LISA, will provide intrinsic sensitivity to both h_+ and h_\times , enabling accurate polarization measurements from a single facility [1, 2].

It is important to note that the two tensor polarizations are frame dependent: a rotation around the propagation axis mixes $h_+(t)$ and $h_\times(t)$. Consequently, observing nonzero values of both components in the detector frame does not necessarily imply that the wave is not linearly polarized. To characterize the polarization in a frame-independent way, we introduce the Stokes parameters [41–44]:

$$\begin{aligned} U &= -2\langle \Re(h_+ h_\times^*) \rangle, \quad V = -2\langle \Im(h_+ h_\times^*) \rangle, \\ I &= \langle |h_+|^2 + |h_\times|^2 \rangle, \quad Q = \langle |h_+|^2 - |h_\times|^2 \rangle. \end{aligned} \quad (24)$$

One can express the metric perturbations in the helicity basis, $h_{R/L} = h_+ \pm i h_\times$, which under a rotation by an angle θ about the propagation axis transform as $h_{R/L} \rightarrow e^{\mp 2i\theta} h_{R/L}$, corresponding to helicities ± 2 . From this, it follows that the Stokes parameters I and V are invariant under rotations, while Q and U are not; however, the combination $\sqrt{Q^2 + U^2}$ is rotationally invariant. A linearly polarized gravitational wave corresponds to a frame in which $U = V = 0$ and $I = Q$. Consequently, $V = 0$ and $\sqrt{Q^2 + U^2} = I$ hold in any reference frame. We can further define the frame-invariant degree

of polarization as

$$P = \frac{\sqrt{Q^2 + U^2 + V^2}}{I}, \quad (25)$$

which in the case of linearly polarized GW gives $P = 1$. This implies that, once $h_+(t)$ and $h_\times(t)$ are reconstructed from the measurement, one can compute the Stokes parameters to characterize the polarization state. A vanishing value of V indicates that the GW is not circularly polarized, while the condition $\sqrt{Q^2 + U^2} = I$ corresponds to a linearly polarized wave. Moreover, a degree of polarization $P = 1$ signifies a fully polarized signal, in this case a fully linearly polarized gravitational wave.

CONCLUSIONS

We have demonstrated that a sufficiently slow first-order phase transition in a radiation-dominated Universe can proceed through the nucleation and collision of only two vacuum bubbles. Under these conditions, the GW signal produced by the bubble collision exhibits linear polarization and can lie within the projected sensitivity of future interferometers, including LISA and the Einstein Telescope. This offers the opportunity of probing such scenarios with future triangular GW detectors, which will be capable of reconstructing the two GW polarizations and, via the application of frame-independent Stokes parameters, identifying the linearly polarized signal. A detection of this polarization signature would provide a unique distinction of such slow transitions relative to other GW production mechanisms, and could deliver direct insights into physics operating in the earliest moments of the Universe. Finally, it would be valuable to complement these analytical results with dedicated numerical simulations. Also, it would be interesting to construct explicit model frameworks capable of realizing such slow first-order phase transitions.

APPENDIX

In the following, we discuss the probability to nucleate only two bubbles in supercooled phase transitions.

In a first-order phase transition, the system may remain temporarily trapped in a metastable false vacuum even after the temperature drops below the critical temperature T_c , where the true and false vacuum are degenerate. When this occurs, the Universe continues to cool while the transition to the true vacuum is delayed, leading to an accumulation of vacuum energy in the false vacuum. This stage, known as supercooling, is characterized by an energy density dominated by the nearly constant false-vacuum component, causing the cosmic expansion to become approximately exponential [23, 30–40]. The resulting behaviour corresponds to a brief, sec-

ondary period of inflation preceding the completion of the phase transition. Thus, the scale factor in this regime is $a(t) \propto e^{Ht}$, where the Hubble rate H is approximately constant. The decay of the false vacuum during supercooling can proceed either through thermal transitions, described by $\Gamma_3(T)$ in Eq. (5), or through quantum tunneling, with decay rate $\Gamma_4 = R_0^{-4} (S_4/2\pi)^2 e^{-S_4}$, where S_4 is the four-dimensional Euclidean action of the $O(4)$ -symmetric bounce solution and R_0 denotes the bubble radius at nucleation. As before, we study the decay rate in a model-independent manner, taking $C(t) = \tilde{C} \cdot T^4$ when $\Gamma_3(T)$ dominates and $C(t) = \tilde{C} \equiv \text{constant}$ when Γ_4 dominates. We define the total number of e-folds of expansion between the critical time t_c and a later time t as

$$N_{\text{tot}}(t) = \int_{t_c}^t dt' H(t') \simeq H(t - t_c). \quad (26)$$

Since the temperature redshifts inversely with the scale factor, $T \propto a(t)^{-1} \propto e^{-Ht}$, the number of e-folds between temperatures T_c and T can be expressed as $N_{\text{tot}}(T) = \ln(T_c/T)$. This quantity measures the total expansion of the Universe during the supercooled stage, before the phase transition completes.

We first consider the case in which quantum tunneling dominates the decay rate. In this regime, we obtain

$$I(t) = \frac{4\pi\tilde{C}v_w^3}{3H^4\beta_H} \left(\frac{6 + 2\beta_H e^{-\beta_H N_{\text{tot}}^* - 3N_{\text{tot}}}}{(1 + \beta_H)(2 + \beta_H)(3 + \beta_H)} - e^{-\beta_H N_{\text{tot}}^*} + \frac{\beta_H^2 - 3e^{N_{\text{tot}}} \beta_H (1 + \beta_H) + 3e^{2N_{\text{tot}}} \beta_H (2 + \beta_H)}{e^{\beta_H N_{\text{tot}}^* + 3N_{\text{tot}}} (1 + \beta_H)(2 + \beta_H)} \right), \quad (27)$$

where we define $N_{\text{tot}}^* \equiv N_{\text{tot}}(t_*)$ and $N_{\text{tot}} \equiv N_{\text{tot}}(t)$. The corresponding expected number of bubbles at completion is given by

$$N(t_*) = \frac{4\pi\tilde{C}}{3H^4} \int_0^{N_{\text{tot}}^*} dN_{\text{tot}} f(N_{\text{tot}}) e^{\beta_H (N_{\text{tot}} - N_{\text{tot}}^*)} e^{-I(t)}, \quad (28)$$

where $f(N_{\text{tot}}) = 1$ for quantum transitions and $f(N_{\text{tot}}) = \exp(-4N_{\text{tot}})$ for thermal transitions, coming from the respective prefactor of the decay rate. Solving $I(t_*) = 4.6$ fixes \tilde{C} , so that Eq. (28) depends only on β_H and N_{tot}^* . We have verified that condition (7) is satisfied for any $\beta_H \geq 1$ and $N_{\text{tot}} > 0$. Moreover, we find that for all $\beta_H \geq 1$ and $N_{\text{tot}} > 0$, $N(t_*) > 3$. Hence, if quantum tunneling dominates, the phase transition always completes with the nucleation of at least three bubbles and the resulting GW signal is not linearly polarized.

For the case dominated by thermal tunneling, we find

$$I(t) = \frac{4\pi\tilde{C}v_w^3}{3H^4 e^{\beta_H N_{\text{tot}}^*}} \left(\frac{6e^{N_{\text{tot}}(\beta_H - 4)}}{(\beta_H - 4)(\beta_H - 3)(\beta_H - 2)(\beta_H - 1)} + \frac{e^{-3N_{\text{tot}}}}{(\beta_H - 1)} - \frac{3e^{-2N_{\text{tot}}}}{(\beta_H - 2)} + \frac{3e^{-N_{\text{tot}}}}{(\beta_H - 3)} - \frac{1}{(\beta_H - 4)} \right) \quad (29)$$

where $\beta_H \in \{1, 2, 3, 4\}$ are removable singularities. In the following analysis, we take $v_w/c = 1$, as bubble walls in the supercooled regime are expected to approach relativistic velocities, being only weakly affected by plasma friction. We find that there exists a function $\bar{\beta}_H(N_{\text{tot}}^*)$ such that, for $\beta_H \geq \bar{\beta}_H(N_{\text{tot}}^*)$, condition (7) is satisfied when $I(t_*) = 4.6$. For any $N_{\text{tot}}^* > 5.7$, there exists a range of β_H with $\bar{\beta}_H(N_{\text{tot}}^*)$ being the lower bound in which the expected number of bubbles per Hubble volume at completion satisfies $2 \leq N(t_*) < 3$ (green region in Fig. 4). For $1 \leq \beta_H < \bar{\beta}_H(N_{\text{tot}}^*)$, the false-vacuum volume is still non-decreasing when $\mathcal{P}_{\text{FV}} \simeq 0.01$, therefore we define the completion time t_* in this regime to correspond to the point at which condition (7) is first satisfied, i.e. $(3H)^{-1}(dI/dt)|_{t=t_*} = 1$. The region of parameter space in which $2 \leq N(t_*) < 3$, in this case, is shown in blue in Fig. 4. The minimal number of e-folds consistent with two-bubble nucleation is $N_{\text{tot},\text{min}}^* = 5.5$.

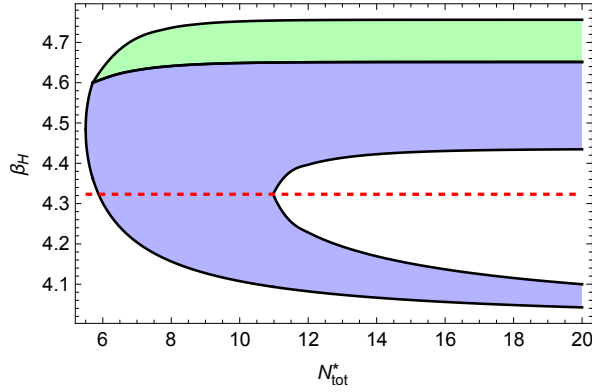


FIG. 4. Parameter space of β_H and N_{tot}^* for which the expected number of bubbles per Hubble volume at completion satisfies $2 \leq N(t_*) < 3$ in a supercooled phase transition. The green region corresponds to cases where the completion time is determined by $I(t_*) = 4.6$, while the purple region denotes the regime where it is set by $(3H)^{-1}dI/dt|_{t=t_*} = 1$. The dashed red line marks $R_*H_* = 1.8$.

For this scenario to hold, we assume that the critical temperature T_c lies below the temperature at which vacuum domination sets in, such that the decay cannot begin during radiation domination. Moreover, consistency of the scenario requires that the thermal tunneling rate increases as the temperature drops below T_c . For temperatures close to the critical point, $T_2 < T_1 \lesssim T_c$, we need

$$\frac{\Gamma_3(T_2)}{\Gamma_3(T_1)} \simeq \exp[(\beta_H - 4)(N_{\text{tot}}(T_2) - N_{\text{tot}}(T_1))] > 1, \quad (30)$$

which implies $\beta_H > 4$. Fig. 4 shows that the parameter space consistent with $2 \leq N(t_*) < 3$ indeed satisfies this bound, though only marginally. This proximity raises concerns about the reliability of this regime.

Using Eq. (11) for the mean bubble size, we find that

at completion $R_*(t_*)H_* \sim 0.9$ within the green region of Fig. 4, making it plausible that bubbles collide when $R_*H_* \sim 0.5$. However, in the purple region above the red dashed line, the mean bubble size is $0.9 < R_*H_* < 1.8$, and below the dashed line one finds $R_*H_* \gg 1$. In this regime a single bubble already spans (or exceeds) the Hubble volume, so the assumption that the transition completes through the collision of two bubbles is no longer self-consistent.

For supercooling to be governed by thermal tunneling, one must verify in any specific model that $\Gamma_3 > \Gamma_4$ up to completion and that the thermal description remains valid, i.e. that the thermalization rate satisfies $\Gamma_{\text{th}} > H^4$.

In conclusion, if quantum tunneling dominates, the transition is expected to end with far more than two bubbles per Hubble volume. When thermal tunneling dominates the supercooled transition, there exists a narrow region of $(\beta_H, N_{\text{tot}}^*)$ in which the transition completes with an average of two bubbles. However, this region lies very close to the boundary of the consistency conditions, and it is unclear whether realistic models can reliably realize such a scenario.

ACKNOWLEDGMENT

I thank Diego Redigolo for pointing me to this question and for valuable discussions. I also thank Lorenzo Ubaldi and Miha Nemevšek for many useful discussions, and Lorenzo Ubaldi in particular for a careful reading of the manuscript and for detailed comments on the draft. I further thank Toby Opferkuch for providing the data of the projected noise curves for the future experiments LISA and ET. This work was supported by the Slovenian Research Agency (research core funding No. P1-0035).

* katarina.trailovic@ijs.si

- [1] A. Abac *et al.* (ET), (2025), [arXiv:2503.12263 \[gr-qc\]](#).
- [2] M. Colpi *et al.* (LISA), (2024), [arXiv:2402.07571 \[astro-ph.CO\]](#).
- [3] B. P. Abbott *et al.* (LIGO Scientific, Virgo), *Phys. Rev. Lett.* **119**, 141101 (2017), [arXiv:1709.09660 \[gr-qc\]](#).
- [4] M. Isi and A. J. Weinstein, (2017), [arXiv:1710.03794 \[gr-qc\]](#).
- [5] H. Takeda, A. Nishizawa, Y. Michimura, K. Nagano, K. Komori, M. Ando, and K. Hayama, *Phys. Rev. D* **98**, 022008 (2018), [arXiv:1806.02182 \[gr-qc\]](#).
- [6] Y. Hagihara, N. Era, D. Iikawa, A. Nishizawa, and H. Asada, *Phys. Rev. D* **100**, 064010 (2019), [arXiv:1904.02300 \[gr-qc\]](#).
- [7] N. Yunes, X. Siemens, and K. Yagi, *Living Rev. Rel.* **28**, 3 (2025).
- [8] R. Abbott *et al.* (LIGO Scientific, VIRGO, KAGRA), *Phys. Rev. D* **112**, 084080 (2025), [arXiv:2112.06861 \[gr-qc\]](#).

- [9] A. Maleknejad, *JHEP* **07**, 104, [arXiv:1604.03327 \[hep-ph\]](#).
- [10] R. R. Caldwell and C. Devulder, *Phys. Rev. D* **97**, 023532 (2018), [arXiv:1706.03765 \[astro-ph.CO\]](#).
- [11] E. Witten, *Phys. Rev. D* **30**, 272 (1984).
- [12] C. J. Hogan, *Mon. Not. Roy. Astron. Soc.* **218**, 629 (1986).
- [13] A. Kosowsky, M. S. Turner, and R. Watkins, *Phys. Rev. D* **45**, 4514 (1992).
- [14] A. Kosowsky, M. S. Turner, and R. Watkins, *Phys. Rev. Lett.* **69**, 2026 (1992).
- [15] M. Kamionkowski, A. Kosowsky, and M. S. Turner, *Phys. Rev. D* **49**, 2837 (1994), [arXiv:astro-ph/9310044](#).
- [16] S. Weinberg, *Gravitation and Cosmology: Principles and Applications of the General Theory of Relativity* (John Wiley and Sons, New York, 1972).
- [17] M. Maggiore, *Gravitational Waves. Vol. 1: Theory and Experiments* (Oxford University Press, 2007).
- [18] S. R. Coleman, *Phys. Rev. D* **15**, 2929 (1977), [Erratum: *Phys.Rev.D* 16, 1248 (1977)].
- [19] A. D. Linde, *Nucl. Phys. B* **216**, 421 (1983), [Erratum: *Nucl.Phys.B* 223, 544 (1983)].
- [20] A. H. Guth and S. H. H. Tye, *Phys. Rev. Lett.* **44**, 631 (1980), [Erratum: *Phys.Rev.Lett.* 44, 963 (1980)].
- [21] A. H. Guth and E. J. Weinberg, *Phys. Rev. D* **23**, 876 (1981).
- [22] M. S. Turner, E. J. Weinberg, and L. M. Widrow, *Phys. Rev. D* **46**, 2384 (1992).
- [23] J. Ellis, M. Lewicki, and J. M. No, *JCAP* **04**, 003, [arXiv:1809.08242 \[hep-ph\]](#).
- [24] P. Athron, C. Balázs, and L. Morris, *JCAP* **03**, 006, [arXiv:2212.07559 \[hep-ph\]](#).
- [25] A. Mégevand and S. Ramírez, *Nucl. Phys. B* **928**, 38 (2018), [arXiv:1710.06279 \[astro-ph.CO\]](#).
- [26] S. R. Coleman and F. De Luccia, *Phys. Rev. D* **21**, 3305 (1980).
- [27] D. Cutting, M. Hindmarsh, and D. J. Weir, *Phys. Rev. D* **97**, 123513 (2018), [arXiv:1802.05712 \[astro-ph.CO\]](#).
- [28] M. Hindmarsh, S. J. Huber, K. Rummukainen, and D. J. Weir, *Phys. Rev. D* **96**, 103520 (2017), [Erratum: *Phys.Rev.D* 101, 089902 (2020)], [arXiv:1704.05871 \[astro-ph.CO\]](#).
- [29] C. Caprini *et al.*, *JCAP* **04**, 001, [arXiv:1512.06239 \[astro-ph.CO\]](#).
- [30] N. Levi, T. Opferkuch, and D. Redigolo, *JHEP* **02**, 125, [arXiv:2212.08085 \[hep-ph\]](#).
- [31] J. Ellis, M. Lewicki, and V. Vaskonen, *JCAP* **11**, 020, [arXiv:2007.15586 \[astro-ph.CO\]](#).
- [32] S. R. Coleman and E. J. Weinberg, *Phys. Rev. D* **7**, 1888 (1973).
- [33] E. Gildener and S. Weinberg, *Phys. Rev. D* **13**, 3333 (1976).
- [34] E. Witten, *Nucl. Phys. B* **177**, 477 (1981).
- [35] T. Hambye and A. Strumia, *Phys. Rev. D* **88**, 055022 (2013), [arXiv:1306.2329 \[hep-ph\]](#).
- [36] S. Iso, P. D. Serpico, and K. Shimada, *Phys. Rev. Lett.* **119**, 141301 (2017), [arXiv:1704.04955 \[hep-ph\]](#).
- [37] A. Azatov, D. Barducci, and F. Sgarlata, *JCAP* **07**, 027, [arXiv:1910.01124 \[hep-ph\]](#).
- [38] L. Randall and G. Servant, *JHEP* **05**, 054, [arXiv:hep-ph/0607158](#).
- [39] G. Nardini, M. Quiros, and A. Wulzer, *JHEP* **09**, 077, [arXiv:0706.3388 \[hep-ph\]](#).
- [40] T. Konstandin and G. Servant, *JCAP* **12**, 009, [arXiv:1104.4791 \[hep-ph\]](#).
- [41] N. Seto and A. Taruya, *Phys. Rev. D* **77**, 103001 (2008), [arXiv:0801.4185 \[astro-ph\]](#).
- [42] G. Gubitosi and J. Magueijo, *Phys. Rev. D* **95**, 023520 (2017), [arXiv:1610.05702 \[gr-qc\]](#).
- [43] R. Kato and J. Soda, *Phys. Rev. D* **93**, 062003 (2016), [arXiv:1512.09139 \[gr-qc\]](#).
- [44] C. Conneely, A. H. Jaffe, and C. M. F. Mingarelli, *Mon. Not. Roy. Astron. Soc.* **487**, 562 (2019), [arXiv:1808.05920 \[astro-ph.CO\]](#).